2016-12-01

Clockwise rotation of the entire Oman ophiolite occurred in a suprasubduction zone setting

Morris, A

10.1130/G38380.1
Geology
Geological Society of America

Morris, A., Meyer, M., Anderson, M. W. and MacLeod, C. J., 2016. Clockwise rotation of the entire Oman ophiolite occurred in response to subduction rollback. Geology, 44, 1055-1058, doi: 10.1130/G38380.

Clockwise rotation of the entire Oman ophiolite occurred in a suprasubduction zone setting

Antony Morris[1], Matthew Meyer[1], Mark W. Anderson[1] and Christopher J. MacLeod[2]

[1]School of Geography, Earth and Environmental Sciences, Plymouth University, Plymouth PL4 8AA, UK
[2]School of Earth & Ocean Sciences, Cardiff University, Cardiff CF10 3AT, UK

ABSTRACT

The Oman ophiolite provides a natural laboratory for understanding oceanic lithospheric processes. Previous paleomagnetic and structural investigations have been used to support a model involving rotation of the ophiolite during formation at a mid-oceanic microplate. However, recent geochemical evidence indicates the ophiolite instead formed in a nascent forearc environment, opening the potential for alternative rotation mechanisms. Central to the conundrum is the contrast between ESE to SE magnetizations and NNW magnetizations from the northern and southern ophiolitic massifs respectively, attributed previously to either differential tectonic rotations during spreading or complete emplacement-related remagnetization of the southern massifs. Here we report new paleomagnetic data from lower crustal rocks of the southern massifs that resolve this problem. Sampling of a continuous section in Wadi Abyad reveals ENE magnetizations in the dike rooting zone at the top of the lower crust that change systematically downwards to NNW directions in underlying foliated and layered gabbros. This is only consistent with remagnetization from the base upwards, replacing early remanences in layered and foliated gabbros completely but preserving original ENE magnetizations at higher levels. Comparison with new data from Wadi Khafifah provides a positive fold test that shows this event occurred before late Campanian structural disruption of the regional orientation of the petrologic Moho. These data show that the entire ophiolite experienced large intraoceanic clockwise rotation prior to partial remagnetization, leading to a new tectonic model in which formation, rotation and emplacement of the ophiolite are all linked to Late Cretaceous motion of Arabia and roll-back of the Oman subduction zone.

Introduction

Paleomagnetic analyses of ophiolites can provide important constraints on tectonic processes in oceanic lithosphere. In particular, paleomagnetic data from Mesozoic ophiolites of the Alpine-Himalayan orogenic belt have demonstrated the importance of tectonic rotation during phases of intraoceanic and/or emplacement-related deformation (e.g. MacLeod et al., 1990; Morris et al., 2002; Inwood et al, 2009; Maffione et al., 2013; Morris and Maffione, 2016). The ~500 km long Oman ophiolite within the Neotethyan suture zone is the largest and most intensively studied ophiolite in the world (e.g. Lippard et al., 1986). It formed at ca. 96 Ma at a fast spreading rate (Nicolas, 1989; MacLeod and Rothery, 1992; Rioux et al., 2012) and was detached soon after formation (Warren et al., 2005), before being emplaced onto the Arabian continental margin by the end of the Cretaceous (Lippard et al., 1986) and subsequently disrupted by gravity-driven extension around basement structural culminations (Cawood et al., 1990). Paleomagnetic studies of the northern massifs of the ophiolite have identified ESE- to SE-directed magnetizations (Fig. 1), indicating large clockwise rotation of (at least) this part of the ophiolite (Shelton, 1984; Thomas et al., 1988; Perrin et al., 1994, 2000; Weiler, 2000). Systematic differences in declination between early (V1, Geotimes unit) and later (V2, Lasail and Alley units)

volcanic units (Perrin et al., 1994, 2000) provide evidence that this rotation began during crustal construction in a pre-emplacement, intraoceanic setting. In contrast, analyses in the southern massifs have identified consistent NNW-directed magnetizations (Fig. 1; Luyendyk et al., 1982; Luyendyk and Day, 1982; Thomas et al., 1988; Feinberg et al., 1999; Weiler, 2000). Together, these data have been used to develop a tectonic model for formation and differential rotation of the ophiolite within a mid-ocean ridge microplate (Boudier et al., 1997) or overlapping spreading center (Weiler, 2000) environment. However, recent geochemical evidence indicates that the ophiolite instead formed in a nascent arc spreading system above a subduction zone immediately following subduction initiation (MacLeod et al., 2013); hence the geodynamic controls driving rotation may be fundamentally different. Furthermore, NNW magnetizations in the southern massifs have also been ascribed to complete late-stage, emplacement-related remagnetization (Feinberg et al., 1999), potentially complicating or even obliterating any earlier magnetic record of intraoceanic rotation in this part of the ophiolite.

Here we present paleomagnetic data from transects through lower crustal rocks of the Oman ophiolite that provide unequivocal evidence that the southern massifs originally held easterly-directed magnetizations, before experiencing subsequent late-stage remagnetization from the base up. This removes ambiguity in the interpretation of the existing paleomagnetic data from Oman, and leads to a new tectonic model involving simple rotation in a suprasubduction zone setting.

Lower crustal geology and paleomagnetic data

Lower oceanic crustal gabbros and underlying mantle peridotites dominate the southern massifs of the Oman ophiolite. We focus on sections in Wadi Abyad (Rustaq massif) and Wadi Khafifah (Ibra massif), where long transects from the Moho through typical lower crustal sequences are exposed (Fig. 1A; Pallister and Hopson, 1981; MacLeod and Yaouancq, 2000). The following lithostratigraphic units were sampled in Wadi Abyad (Fig. 1B): (i) layered gabbros in the lower half of the section (Fig. DR1 in the GSA Data Repository), with layering defined principally by modal variations in olivine, clinopyroxene and plagioclase on a cm to m scale. Layering is consistently sub-parallel to the NNE-dipping Moho (Fig, DR2), the orientation of which (Table DR1) provides a paleohorizontal surface for tilt correction of the paleomagnetic data; (ii) foliated gabbros (Fig. DR3), with preferred mineral orientations defining a consistently steep, near Moho-perpendicular foliation and a sub-vertical lineation; (iii) varitextured gabbros (Fig. DR4), marked by high variability in grain size, texture and composition over short distances (and locally cut by discrete dikes), that represent the fossil axial melt lens (MacLeod and Yaouancq, 2000); and (iv) the dike rooting zone, that has a gradational contact with the underlying varitextured gabbros and that consists of microgabbro and basalt dikes separated by gabbro screens (Fig. DR5). Layered and foliated gabbros with the same characteristics were also sampled in Wadi Khafifah (Fig. DR6), but here the Moho dips to the south (Table DR1), allowing a regional-scale fold test to be performed between localities.

Oriented paleomagnetic cores collected at 19 sites along Wadi Abyad and at 13 sites along Wadi Khafifah were analysed using standard paleomagnetic laboratory techniques (see Data Repository). Following removal of occasional low stability, present field viscous components, demagnetization data define either linear, single components of magnetization or, in the case of varitextured gabbro samples in Wadi Abyad, curvilinear trajectories leading to linear components at high treatment levels (Fig. DR7). In all cases, laboratory unblocking temperatures close to 580°C and supporting rock magnetic experiments indicate that these remanences are carried by nearly stoichiometric magnetite (Figs. DR8 and DR9). All sites yielded statistically well-defined mean magnetization vectors (Table DR1) that have a consistent normal polarity (positive inclinations) after tilt

correction. In both Wadi Abyad and Wadi Khafifah, layered and foliated gabbros overall display NNW-directed magnetizations (Fig. 1C; Fig. DR6). This is consistent with data reported previously from one layered gabbro site in each of these sections by Weiler (2000). However, sampling of the complete crustal section shows that site mean magnetizations in the Wadi Abyad foliated gabbros vary systematically from NNW directions in the lowermost sites to north directions in the uppermost sites, passing upwards into varitextured gabbros with distributed NE-directed magnetizations, and finally into the dike rooting zone marked by ENE remanences (Fig. 1C).

Origin and timing of magnetizations

ENE-directed, normal polarity magnetization directions at the top of the lower crust in Wadi Abyad require clockwise vertical axis rotation of the section. The distribution of site directions beneath, however, can only be explained by remagnetization from the base upwards via production of secondary magnetite during fluid-mediated alteration, with pervasive overprinting of the base of the section decreasing progressively upwards to preserve original ENE magnetizations at the top. This is supported by the following evidence: (i) curvilinear demagnetization paths in the varitextured gabbros (Fig. DR7) suggest significant overlap in unblocking temperature or coercivity spectra of two different magnetization components, consistent with the presence of a magnetic overprint superimposed on an original thermoremanence; (ii) demagnetization data at lower treatment levels in the varitextured gabbros define great circle paths that trend towards the magnetization direction of the foliated and layered gabbros beneath (Fig. 1). The magnetic overprint in these rocks hence shares the same direction as the NNW-directed characteristic magnetization seen lower in the section; and (iii) petrographic evidence that shows a dominance of secondary magnetite in the layered and foliated gabbros, mainly associated with serpentinization of olivine, and mostly primary magnetite in the varitextured and dike rooting zone gabbros (Yaouancq and MacLeod, 2000; Meyer, 2015). This can account for observed variations in magnetization directions in both the foliated and varitextured gabbros, which may be attributed to between-site variations in the relative proportions of primary and secondary magnetite and in the degree of overlap of their blocking temperature or coercivity spectra.

Remagnetization of the southern blocks of the ophiolite has been invoked previously by Feinberg et al. (1999) on the basis of comparison of paleomagnetic data from seven sites in mantle peridotites and two sites in layered gabbros with those obtained from five sites in high-grade continental metabasites underlying the ophiolite. NNW magnetizations with shallow inclinations in the metabasites were interpreted as thermochemical remanences acquired during exhumation and cooling from peak metamorphic conditions between 80 and 70 Ma. Observation of identical directions of magnetization in overlying serpentinized peridotites and layered gabbros led Feinberg et al. (1999) to infer contemporaneous remagnetization of the ophiolite via alteration associated with upward advection of metamorphic fluids in the faulted ophiolite. This interpretation is entirely consistent with our new data, which independently demonstrate that remagnetization of the ophiolite occurred from the base upwards. Preservation of ENE magnetizations in the Wadi Abyad dike rooting zone defines the upper limit of fluid advection at this locality, although NNW remanences reported from dikes of the Ibra massif (Fig. 1; Luyendyk et al., 1982) suggest that remagnetization elsewhere extended further up into the sheeted dike complex.

The timing of remagnetization of the southern massifs may be constrained by comparing paleomagnetic data from Wadis Abyad and Khafifah, as variations in the orientation of the Moho between these locations allow a paleomagnetic fold test to be performed. Upon restoration to the paleohorizontal, site mean directions from layered and foliated gabbros at these localities converge (Fig. DR10A & B). A bootstrap statistical test

(Tauxe & Watson, 1994) indicates that the tightest grouping occurs at close to 100% untilting (94-116%; Fig. 1D; Fig. DR10C), constituting a positive fold test. Hence remanences were acquired prior to structural disruption of the regional orientation of the Moho that occurred during gravitational sliding away from emerging basement structural highs in the Campanian (Cawood et al., 1990). Combined with the preservation of demonstrably older (and presumed primary, ridge-related) remanences in the Wadi Abyad dike rooting zone, this is consistent with remagnetization during emplacement of the structurally intact ophiolite sheet onto the Arabian margin.

The lowermost three layered gabbro sites in Wadi Abyad (WA09-WA11; Table DR1) have tilt corrected magnetizations that differ from the rest of the data from this section (Fig. 1). However, their *in situ* magnetizations are indistinguishable from tilt corrected directions observed in layered and foliated gabbros higher up the section. This implies that these sites acquired their magnetizations later in the deformation history than the rest of the section, potentially indicating that the lowest part of the sequence became remagnetized during the waning stages of fluid migration, after significant tilting of the section.

Implications for the tectonic evolution of the Oman ophiolite

Identification in Wadi Abyad of two significantly different remanence directions that both pre-date deformation of the Moho provides critical constraints on the rotation history of the southern massifs and their relationship to the northern massifs. Comparison of the mean tilt corrected magnetization of the foliated and layered gabbros (excluding sites WA09-WA11; Table DR1) with a reference direction derived from the 70 Ma African apparent polar wander path (Torsvik et al., 2012) requires 22°±7° of counterclockwise rotation after remagnetization (Demarest, 1983). Back-stripping the effect of this rotation from the pre-remagnetization direction of the dike rooting zone then indicates an earlier clockwise rotation of 87°±11°. This demonstrates that the southern massifs experienced a clockwise rotation along with the northern massifs (Shelton, 1984; Thomas et al., 1988; Perrin et al., 1994, 2000; Weiler, 2000), and removes the need for large differential rotations within the ophiolite that otherwise require complex tectonic models (Weiler, 2000).

Given paleomagnetic evidence for active rotation during crustal accretion (Perrin et al., 1994, 2000) and geochemical evidence for formation of the ophiolite above an intraoceanic subduction zone (e.g. MacLeod et al., 2013), the recognition of ophiolite-wide, pre-remagnetization clockwise rotation is consistent with a simple tectonic model (Fig. 2) involving: (i) impingement of the Arabian continental margin with a young intraoceanic subduction zone that begins to roll-back, resulting in suprasubduction zone spreading and early rotation of newly-formed crust; (ii) continued northward movement of Arabia and accompanying roll-back of the Oman subduction zone system, leading to further rotation and eventually to emplacement of the rotated ophiolite onto the Arabian margin; (iii) impingement of the southern massifs with basement structural highs (Saih Hatat), triggering a wave of orogenic fluids, near wholesale remagnetization from the base up and subsequent back-rotation; and (iv) extensional collapse generating the present-day configuration of the ophiolite.

This model is consistent with a conceptual framework for rotation in modern subduction systems undergoing collision with buoyant indenters proposed by Wallace et al. (2005) on the basis of plate kinematics in the Pacific region. In these systems a combination of indentation and subduction roll-back generates a torque on the upper plate, leading to rapid rotation of forearc regions (Wallace et al., 2005). In this context, we note that clockwise rotation of the Oman ophiolite mirrors the c. 90° counterclockwise rotation of the Troodos and Hatay ophiolites in the southern Neotethys ocean to the west of the Arabian margin (Clube et al., 1985; Inwood et al., 2009). Rotation of these ophiolites

similarly occurred prior to emplacement, in response to impingement of the Arabian indenter with the southern Neotethyan subduction zone.

ACKNOWLEDGEMENTS
We thank Mohamed Alaraimi (Sultanate of Oman Ministry of Commerce and Industry, Directorate General of Minerals) for permission to undertake field sampling in Oman. The bootstrap fold test was performed using PmagPy software (Tauxe et al., 2010). We thank Gabriel Gutiérrez-Alonso, Phil McCausland and Eric Ferre for constructive reviews.

REFERENCES CITED

Boudier, F., Nicolas, A., Ildefonse, B., and Jousselin, D., 1997. EPR microplates, a model for the Oman Ophiolite: Terra Nova, v.9, p. 79-82.

Cawood, P. A., Green, F. K. and Calon, T. J., 1990. Origin of culminations within the Southeast Oman Mountains at Jebel Majhool and Ibra Dome. In: Robertson, A. H. F., Searle, M. P. and Ries, A. C. (eds.). The Geology and Tectonics of the Oman Region. Geological Society of London Special Publication, v. 49, p. 429-445.

Clube, T. M. M., Creer, K. M. and Robertson, A. H. F., 1985, Palaeorotation of the Troodos microplate, Cyprus: Nature, v. 317, p. 522-525.

Demarest, Jr., H. H., 1983. Error analysis for the determination of tectonic rotation from paleomagnetic data: Journal of Geophysical Research, v. 88, p. 4321-4328.

Feinberg, H., Horen, H., Michard, A. and Saddiqi, O., 1999. Obduction-related remagnetization at the base of an ophiolite: Paleomagnetism of the Samail nappe lower sequence and of its continental substratum, southeast Oman Mountains: Journal of Geophysical Research, v. 104 (B8), p. 17,703-17,714.

Inwood, J., Morris, A., Anderson, M. W. and Robertson, A. H. F., 2009. Neotethyan intraoceanic microplate rotation and variations in spreading axis orientation: Palaeomagnetic evidence from the Hatay ophiolite (southern Turkey): Earth and Planetary Science Letters, v. 280, p. 105-117.

Lippard, S. J., Shelton, A. W. and Gass, I., 1986. The Ophiolite of Northern Oman, Geological Society, of London Memoir 11, 178 p.

Luyendyk, B. P. and Day, R., 1982. Paleomagnetism of the Samail ophiolite, Oman. 2. The Wadi Kadir gabbro section: Journal of Geophysical Research, v. 87 (B13), p. 10,903-10,917.

Luyendyk, B. P., Laws, B. R., Day, R. and Collinson, T. B., 1982. Paleomagnetism of the Samail ophiolite, Oman. 1. The sheeted dike complex at Ibra: Journal of Geophysical Research, v. 87 (B13), p. 10,883-10,902.

MacLeod, C. J. and Rothery, D. A., 1992. Ridge axial segmentation in the Oman ophiolite: evidence from along-strike variations in the sheeted dyke complex, in Parson, L. M., Murton, B. J., and Browning, P., eds., Ophiolites and their modern oceanic analogues: Geological Society of London Special Publication, v. 60, p. 39-63.

MacLeod, C. J. and Yaouancq, G., 2000. A fossil melt lens in the Oman ophiolite: Implications for magma chamber processes at fast spreading ridges: Earth and Planetary Science Letters, v. 176, p. 357-373.

MacLeod, C.J., Allerton, S., Gass I.G. and Xenophontos, C., 1990. Structure of a fossil ridge-transform intersection in the Troodos ophiolite: Nature, v. 348, p. 717-720.

MacLeod, C. J., Lissenberg, C. J. and Bibby, L. E., 2013. “Moist MORB” axial magmatism in the Oman ophiolite: The evidence against a mid-ocean ridge origin: Geology, v. 41, p. 459-462

Maffione, M., Morris, A., and Anderson, M. W., 2013, Recognizing detachment-mode spreading in the deep geological past: Scientific Reports, 3:2336, doi: 10.1038/srep02336.

Meyer, M. C., 2015, Magnetic fabric, palaeomagnetic and structural investigation of the accretion of lower oceanic crust using ophiolitic analogues [Ph.D. thesis]: University of Plymouth, 305 pp.

Morris, A., and Maffione, M., 2016, Is the Troodos ophiolite (Cyprus) a complete, transform fault-bounded Neotethyan ridge segment?: Geology, v. 44, p. 199-202, doi: 10.1130/G37529.1.

Morris, A., Anderson, M. W., Robertson, A. H. F., and Al-Riyami, K., 2002, Extreme tectonic rotations within an eastern Mediterranean ophiolite (Baër-Bassit, Syria): Earth and Planetary Science Letters, v. 202, p. 247-261.

Nicolas, A., 1989. Structures of Ophiolites and Dynamics of Oceanic Lithosphere. Kluwer Academic Publishers, Dordrecht, 367pp.

Pallister, J. S. and Hopson, C. A., 1981. Samail Ophiolite Plutonic Suite: Field Relations, Phase Variations, Cryptic Variation and Layering, and a Model of a Spreading Ridge Magma Chamber: Journal of Geophysical Research, v. 86 (B4), p. 2593-2644.

Perrin, M., Prevot, M. and Bruere, F., 1994. Rotation of the Oman ophiolite and initial location of the ridge in the hotspot reference frame: Tectonophysics, v. 229, p. 31-42.

Perrin, M., Plenier, G., Dautria, J.-M., Cocuaud, E. and Prévot, M., 2000. Rotation of the Semail ophiolite (Oman): Additional paleomagnetic data from the volcanic sequence: Marine Geophysical Researches, v. 21, p. 181-194.

Rioux, M., Bowring, S., Kelemen, P., Gordon, S., Dudás, F. and Miller, R., 2012. Rapid crustal accretion and magma assimilation in the Oman-U.A.E. ophiolite: High precision U-Pb zircon geochronology of the gabbroic crust: Journal of Geophysical Research, v. 117, B07201, doi: 10.1029/2012JB009273.

Shelton, A. W., 1984. Geophysical studies on the northern Oman Ophiolite [Ph.D. Thesis]: Milton Keynes, UK, The Open University, 353 p.

Tauxe, L., and Watson, G. S., 1994, The fold test: an eigen analysis approach: Earth and Planetary Science Letters, v. 122, p. 331-341.

Tauxe, L., Butler, R. F., Banerjee, S. K., and Van der Voo, R. (2010). *Essentials of paleomagnetism*. University of California Press, Berkeley. 500 pp.

Thomas, V., Pozzi, J. P. and Nicolas, A., 1988. Paleomagnetic results from Oman ophiolites related to their emplacement: Tectonophysics, v. 151, p. 297-321.

Torsvik, T. H., Van der Voo, R., Preeden, U., Mac Niocaill, C., Steinberger, B., Doubrovine, P. V., van Hinsbergen, D. J., Domeier, M., Gaina, C., and Tohver, E., 2012, Phanerozoic polar wander, palaeogeography and dynamics: Earth-Science Reviews, v. 114, p. 325-368.

Wallace, L. M., McCaffrey, R., Beavan, J. and Ellis, S., 2005. Rapid microplate rotations and backarc rifting at the transition between collision and subduction: Geology, v. 33, p. 857-860, doi: 10.1130/G21834.1.

Warren, C., Parrish, R., Waters, D. and Searle, M., 2005. Dating the geologic history of Oman's Semail ophiolite: Insights from U-Pb geochronology: Contrib. Mineral. Petrol., v. 150 (4), p. 403–422.

Weiler, P. D., 2000. Differential rotations in the Oman ophiolite: paleomagnetic evidence from the southern massifs: Marine Geophysical Researches, v. 21, p. 195-210.

Yaouancq, G. and MacLeod, C. J., 2000. Petrofabric Investigation of Gabbros from the Oman Ophiolite: Comparison between AMS and Rock Fabric: Marine Geophysical Researches, v. 21, p. 289-305.

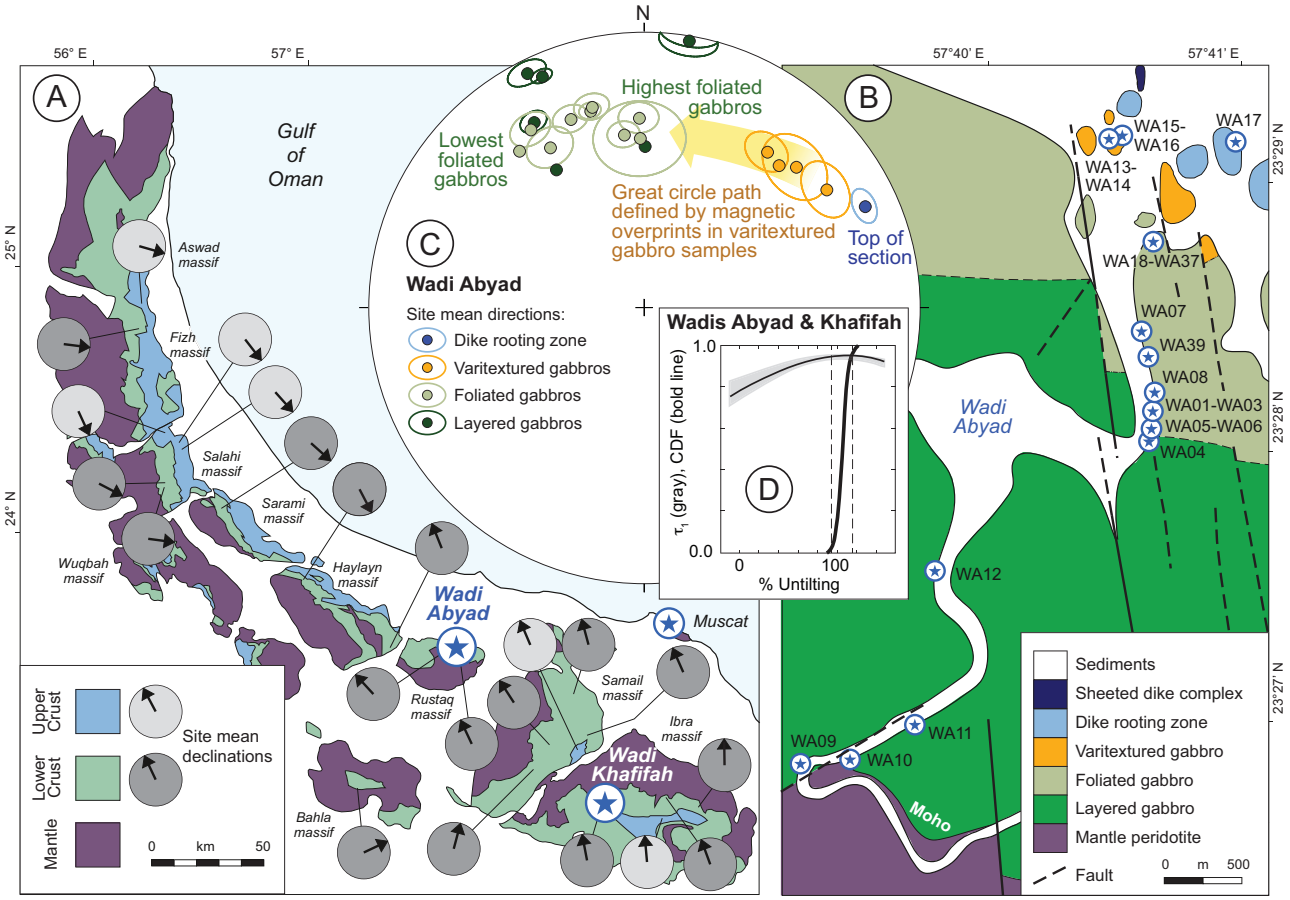

Figure 1. A: Simplified geological map of the Oman ophiolite, showing the location of the ophiolitic massifs and a summary of paleomagnetic declinations obtained from crustal rocks in previous studies (Luyendyk & Day, 1982; Shelton, 1984; Thomas, 1988; Perrin *et al.*, 1994, 2000; Weiler, 2000). Note contrasting ESE and SE versus NNW magnetization directions in the northern and southern massifs, respectively. B: Geological map of Wadi Abyad, showing location of sampling sites (blue stars) distributed through the lower crustal sequence. C: Equal area projection showing tilt corrected site mean magnetization directions from Wadi Abyad and their associated α_{95} cones of confidence (ellipses). Note the progressive change in magnetization directions upwards through the sampled section. D: Positive bootstrap fold test (Tauxe and Watson, 1994) demonstrating that the remagnetization of layered and foliated gabbros in Wadi Abyad and Wadi Khafifah occurred prior to tilting of the Moho in these sections. Gray region contains the trends of the largest eigenvalues (τ_1s) of orientation matrices from representative pseudo-samples during progressive untilting. Bold line is cumulative distribution function (CDF) of 1000 maxima of τ_1 and dashed lines are the bounds that enclose 95% of them.

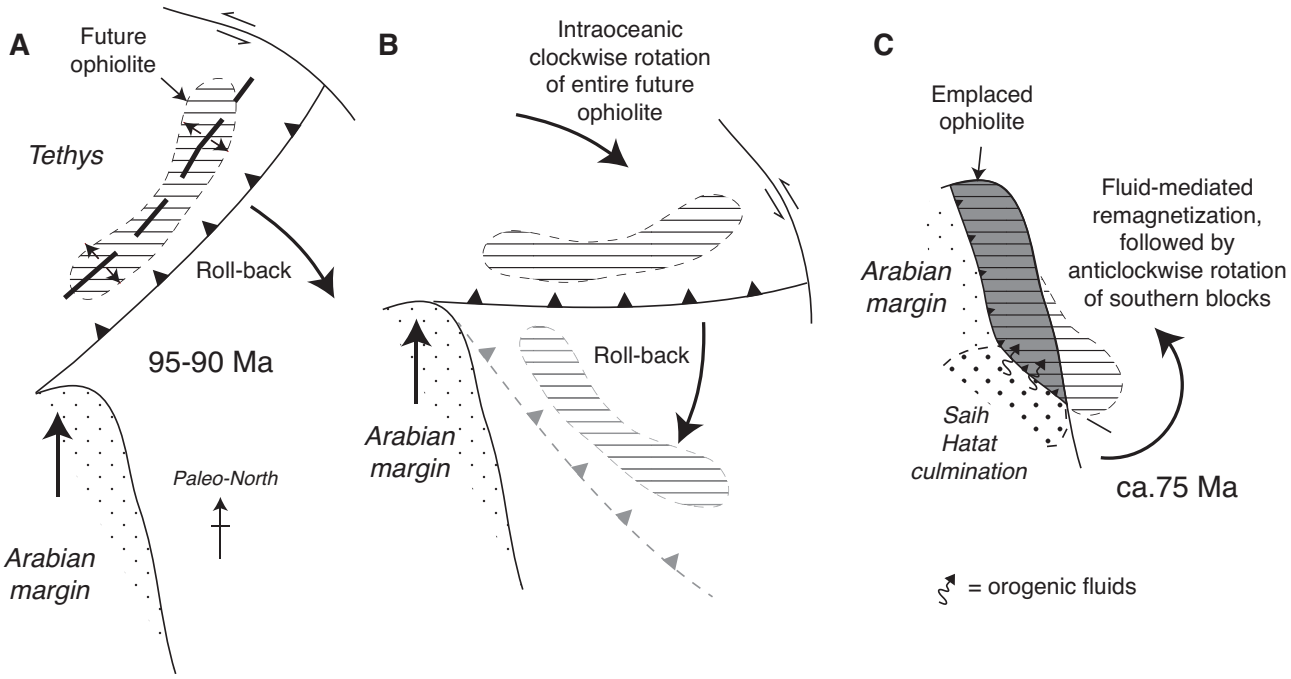

Figure 2. Schematic model for rotation of the Oman ophiolite: (a) formation by spreading along a northeast-southwest-oriented axis and synchronous early rotation in response to a torque due to impingement of the Arabian margin with the subduction zone and subduction roll-back to the east; (b) continued clockwise rotation driven by further northward movement of Arabia and further roll-back; and (c) eventual emplacement of the ophiolite on the Arabian margin, with remagnetization and anticlockwise back rotation of the southern blocks driven by the development of the Saih Hatat structural culmination.

DATA REPOSITORY – METHODS

Oriented samples were collected in the field, either as 25 mm diameter cores using a standard paleomagnetic rock drill or as oriented hand samples from which cores were prepared in the laboratory. Natural remanent magnetizations (NRMs) of samples were investigated via either alternating field demagnetization using an AGICO LDA-3A demagnetizer in 15 incremental steps from 5 to 100 mT, or via thermal demagnetization using a Magnetic Measurements Ltd MMTD80A furnace in 16 temperature increments from 100 to 580°. Magnetic remanences were measured at each demagnetization step using an AGICO JR-6A spinner magnetometer. Demagnetization data were displayed on orthogonal vector plots (Zijderveld, 1967), and remanence components were isolated via principal component analysis (Kirschvink, 1980) using Remasoft 3.0 software (Chadima and Hrouda, 2006). Thermal and AF demagnetization of samples yielded the same directions at each site (Fig. DR7). Site mean directions were evaluated using Fisherian statistics (Fisher, 1953) on virtual geomagnetic poles (VGPs) corresponding to the isolated characteristic remanent magnetizations (ChRMs). The errors ΔD and ΔI associated with the mean declination and inclination at each site are calculated after Deenen et al. (2011) from the VGPs based on the paleolatitude (λ) and the A_{95} values, where:

$$\Delta D = \sin^{-1}(\sin(A_{95})/\cos(\lambda))$$

$$\Delta I = 2A_{95}/(1+3\sin^2(\lambda))$$

The VGP scatter (i.e., A_{95}) obtained at each site was compared to the expected scatter induced by paleosecular variation (PSV) of the geomagnetic field (i.e., A_{95min} - A_{95max}) to assess whether PSV is sufficiently represented in our datasets (Deenen et al., 2011). Values of $A_{95} < A_{95min}$ at 30 out of 32 sites indicate that PSV is not adequately represented, most likely as a result of complete remagnetization or the influence of residual overprints after demagnetization. The remaining two sites have $A_{95min} \approx A_{95} < A_{95max}$ indicating marginal but statistically significant averaging of PSV at site level.

DATA REPOSITORY – REFERENCES

Chadima, M., Hrouda, F., 2006, Remasoft 3.0 a user-friendly paleomagnetic data browser and analyzer. Travaux Géophysiques v. XXVII, p. 20–21.

Deenen, M. H. L., Langereis, C. G., van Hinsbergen, D. J. J., and Biggin, A. J., 2011, Geomagnetic secular variation and the statistics of palaeomagnetic directions: Geophysical Journal International, v. 186, p. 509-520.

Fisher, R. A., 1953, Dispersion on a sphere: Proc. R. Soc. London, v. 217, p. 295-305.

Kirschvink, J. L., 1980, The least-squares line and plane and the analysis of palaeomagnetic data: Geophysical Journal, Royal Astronomical Society, v. 62, p. 699-718.

MacLeod, C. J. and Yaouancq, G., 2000. A fossil melt lens in the Oman ophiolite: Implications for magma chamber processes at fast spreading ridges, Earth and Planetary Science Letters, v. 176, p. 357-373.

Petrovský, E., and Kapička, A., 2006, On determination of the Curie point from thermomagnetic curves: Journal of Geophysical Research, v. 111, B12S27, doi:10.1029/2006JB004507.

Tauxe, L., and Watson, G. S., 1994, The fold test: an eigen analysis approach: Earth and Planetary Science Letters, v. 122, p. 331-341.

Zijderveld, J. D. A., 1967, AC demagnetization of rocks: Analysis of results: Methods in Paleomagnetism, p. 254-286.

DATA REPOSITORY – TABLE & FIGURES

Site	Latitude (°N)	Longitude (°E)	In situ Dec	In situ Inc	Tilt corrected Dec	Tilt corrected Inc	ΔD	ΔI	k	α_{95}	K	A_{95}	A_{95min}	A_{95max}	N
Wadi Abyad (Moho orientation for tilt correction = 032/32)															
Layered gabbros:															
WA09	23° 26' 39.4"	57° 39' 13.0"	005.3	31.3	009.4	2.1	5.9	11.8	113.9	6.3	129.8	5.9	8.3	26.5	6
WA10	23° 26' 41.7"	57° 39' 27.1"	327.2	25.3	336.1	9.1	2.2	4.4	498.8	2.5	623.4	2.2	7.4	22.1	8
WA11	23° 26' 49.8"	57° 39' 41.8"	326.6	20.9	333.4	5.5	4.3	8.6	149.2	4.5	164.4	4.3	7.4	22.1	8
WA12	23° 27' 24.2"	57° 39' 48.1"	296.7	46.1	327.4	40.2	2.1	2.7	1310.2	1.9	1167.1	2.0	8.3	26.5	6
WA04	23° 27' 52.6"	57° 40' 37.3"	312.6	33.4	329.2	22.7	3.1	5.3	119.9	3.5	162.5	3.0	5.8	14.9	15
Foliated gabbros:															
WA05	23° 27' 54.5"	57° 40' 38.1"	302.0	33.6	321.4	28.0	1.3	2.1	1853.9	1.3	1896.3	1.3	7.4	22.1	8
WA06	23° 27' 54.5"	57° 40' 37.1"	309.9	33.8	327.4	24.3	4.8	8.2	105.2	5.4	138.5	4.7	7.4	22.1	8
WA01	23° 27' 57.9"	57° 40' 38.7"	318.4	42.2	338.6	27.4	4.5	7.3	170.9	4.6	194.0	4.3	7.8	24.1	7
WA02	23° 27' 57.9"	57° 40' 38.7"	324.6	44.7	344.6	26.9	2.1	3.5	394.7	2.8	720.5	2.1	7.4	22.1	8
WA03	23° 27' 57.9"	57° 40' 38.7"	326.2	44.0	345.3	25.7	3.0	5.1	181.7	4.5	421.9	2.9	7.8	24.1	7
WA08	23° 28' 3.6"	57° 40' 39.4"	305.1	41.8	329.5	33.0	5.2	7.7	208.2	6.4	344.8	5.0	9.8	34.2	4
WA39	23° 28' 10.7"	57° 40' 39.4"	329.4	60.8	358.4	38.4	9.9	13.1	39.5	12.3	70.1	9.2	8.9	29.7	5
WA07	23° 28' 16.6"	57° 40' 36.1"	336.3	55.2	358.3	31.7	4.6	7.0	115.2	5.2	159.0	4.4	7.4	22.1	8
WA18-37	23° 28' 35.5"	57° 40' 38.2"	324.8	57.1	353.2	36.9	4.0	5.5	31.1	4.3	40.1	3.8	4.0	8.4	37
Varitextured gabbros:															
WA13	23° 29' 2.6"	57° 40' 27.5"	069.5	50.2	056.9	22.5	7.6	13.3	105.2	7.5	105.4	7.5	8.9	29.7	5
WA14 (discrete dike)	23° 29' 2.6"	57° 40' 27.5"	052.2	60.8	043.2	29.8	1.6	2.5	1790.9	1.8	2402.4	1.6	8.9	29.7	5
WA15	23° 29' 1.5"	57° 40' 26.0"	056.9	56.3	047.0	26.0	10.1	16.8	36.0	9.4	33.0	9.8	7.4	22.1	8
WA16 (discrete dike)	23° 29' 1.5"	57° 40' 26.0"	042.9	60.6	038.1	28.9	6.4	10.2	59.2	6.0	55.1	6.2	6.5	18.1	11
Dike-rooting zone:															
WA17	23° 28' 57.8"	57° 40' 55.4"	075.0	38.8	065.2	13.2	3.3	6.3	171.3	4.2	287.0	3.3	7.4	22.1	8
Wadi Khafifah (Moho orientation for tilt correction = 173/29)															
Layered gabbros:															
KF03	22° 52' 19.4"	58° 25' 45.8"	340.9	-8.3	340.2	20.1	5.6	10.0	45.2	7.7	89.0	5.5	7.1	20.5	9
KF04	22° 53' 35.6"	58° 25' 24.4"	358.0	1.4	358.8	30.2	1.9	2.9	880.9	1.9	928.0	1.8	7.4	22.1	8
KF05	22° 53' 35.6"	58° 25' 24.5"	000.0	-3.0	000.9	25.7	3.6	6.1	306.8	3.8	359.5	3.5	8.3	26.5	6
KF06	22° 53' 35.6"	58° 25' 24.5"	359.7	-3.6	000.4	25.2	2.4	4.1	498.2	3.0	814.6	2.3	8.3	26.5	6
KF08	22° 53' 36.3"	58° 25' 29.1"	355.2	7.8	355.8	36.8	2.8	3.9	149.2	2.7	151.4	2.7	5.1	12.4	20
Foliated gabbros:															
KF02	22° 51' 0.3"	58° 24' 57.0"	333.2	10.5	328.2	37.4	8.8	11.9	69.4	9.3	87.4	8.2	8.9	29.7	5
KF10	22° 50' 16.5"	58° 25' 34.0"	334.7	-11.6	334.4	15.9	2.1	3.9	911.4	2.5	1366.1	2.1	8.9	29.7	5
KF11	22° 50' 16.5"	58° 25' 34.1"	330.2	-1.9	327.7	24.7	1.7	2.9	883.7	2.6	1639.9	1.7	8.3	26.5	6
KF12-27	22° 51' 0.4"	58° 24' 57.5"	336.9	6.9	333.5	34.6	3.5	5.0	30.3	3.6	37.0	3.3	3.5	6.8	52
KFS01	22° 49' 51.2"	58° 25' 19.5"	328.2	-10.2	327.6	16.2	5.3	9.9	37.6	9.1	111.9	5.3	7.4	22.1	8
KFS02	22° 49' 52.5"	58° 25' 19.1"	332.0	-3.9	330.1	23.1	2.1	3.6	326.2	3.1	728.5	2.1	7.4	22.1	8
KFS03	22° 49' 53.3"	58° 25' 18.3"	350.3	13.1	349.4	42.0	4.3	5.2	415.8	3.3	290.5	3.9	8.3	26.5	6
KFS04	22° 49' 55.8"	58° 25' 16.5"	324.7	1.9	320.8	27.1	2.8	4.5	184.5	3.4	293.0	2.7	6.5	18.1	11

Table DR1. Paleomagnetic results from Wadi Abyad and Wadi Khafifah, Oman ophiolite. Moho orientation is expressed as dip direction/dip. Dec = site mean declination. Inc = site mean inclination. ΔD, ΔI, declination and inclination error, respectively. k, α_{95}, precision parameter and 95% cone of confidence around the site mean characteristic remanent magnetizations (ChRMs) after Fisher (1953). K, A_{95}, precision parameter and 95% cone of confidence around the site mean virtual geomagnetic pole (VGP). A_{95min}, A_{95max}, minimum and maximum value of A_{95} expected from paleosecular variation (PSV) of the geomagnetic field, according to Deenen et al. (2011). N, number of total samples used for the statistics.

Figure DR1. Typical exposure of layered gabbros in Wadi Abyad, Oman.

Figure DR2. The petrological Moho exposed in Wadi Abyad, Oman. Mantle peridotites at the base of the section are overlain by modally layered gabbros. Layering is clearly visible in the upper right of the photograph, and is oriented parallel to the sharp boundary between crustal and mantle rocks (crossing the centre of the photograph).

Figure DR3. Foliated gabbros exposed in Wadi Abyad, Oman. Note the steep orientation of the prominent magmatic foliation.

Figure DR4. Varitextured gabbros exposed in Wadi Abyad, Oman, representing the fossil axial melt lens of the Oman spreading axis (MacLeod and Yaouancq, 2000).

Figure DR5. Exposure of the dike rooting zone at the top of the Wadi Abyad section, Oman. Note the steeply dipping magmatic contact (to the left of the compass-clinometer), between a basaltic dike and the surrounding gabbro (right and left hand sides of the photograph, respectively).

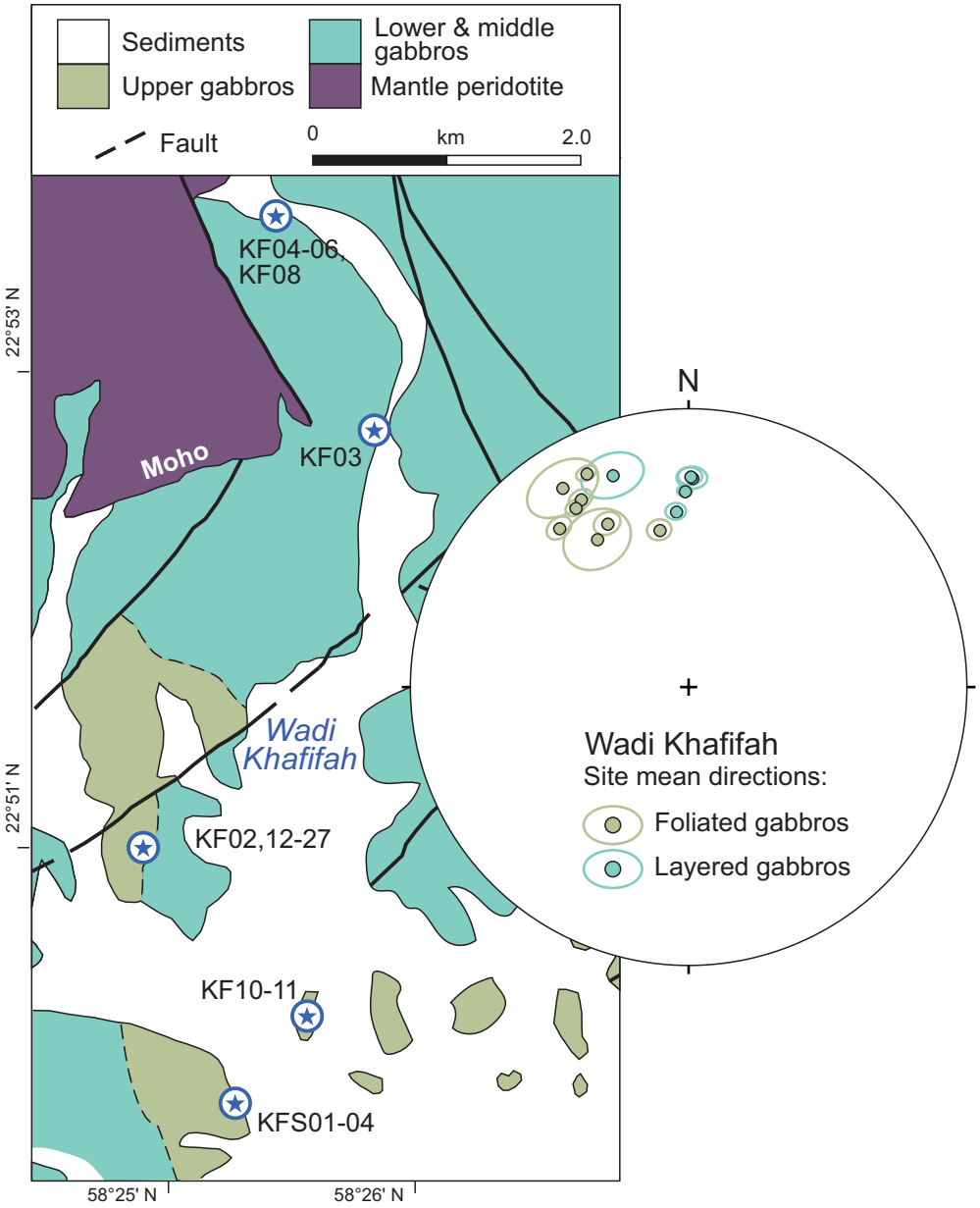

Figure DR6. Geological map of Wadi Khafifah, showing location of sampling sites. Inset: Lower hemisphere equal area projection of tilt corrected site mean magnetization directions and associated α_{95} cones of confidence (ellipses).

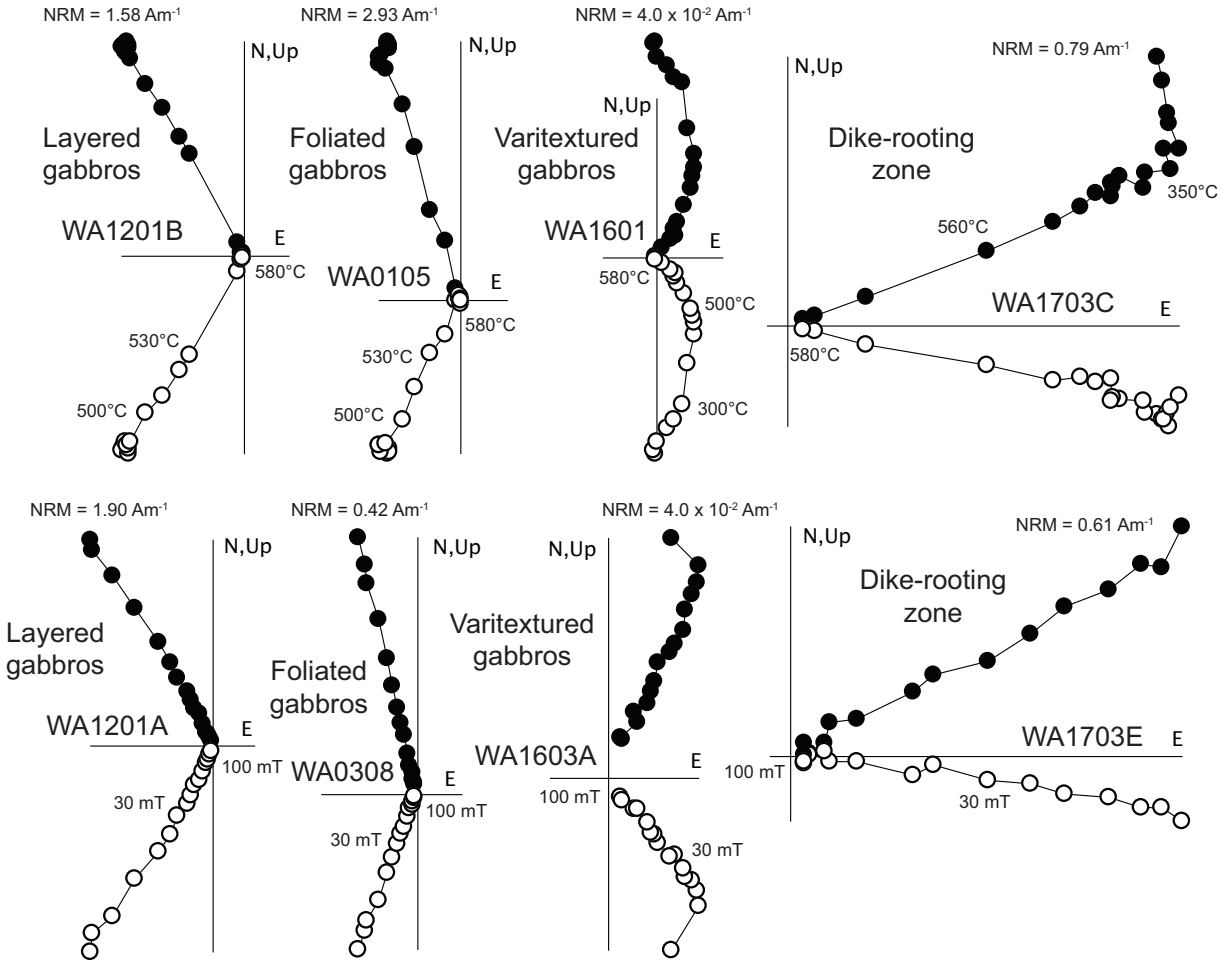

Figure DR7. Representative tilt corrected orthogonal vector plots of thermal (top) and alternating field (bottom) demagnetization data from specimens from different crustal levels in Wadi Abyad. Solid/open circles are projections of the remanence vector onto the horizontal/vertical planes respectively.

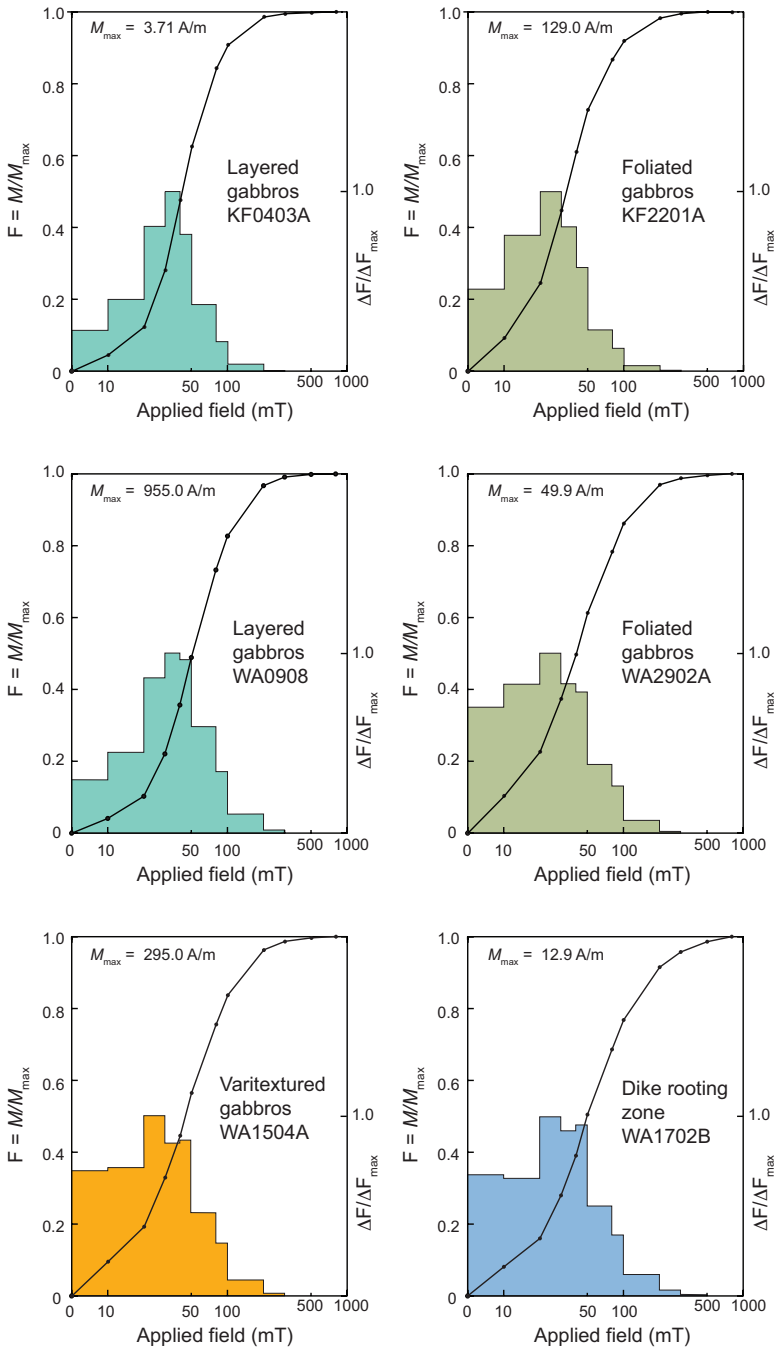

Figure DR8. Representative examples of isothermal remanent magnetization acquisition curves for lower crustal rocks from Wadi Abyad (WA) and Wadi Khafifah (KF) in the Oman ophiolite, showing saturation by 300 mT consistent with remanence carried by low coercivity magnetite.

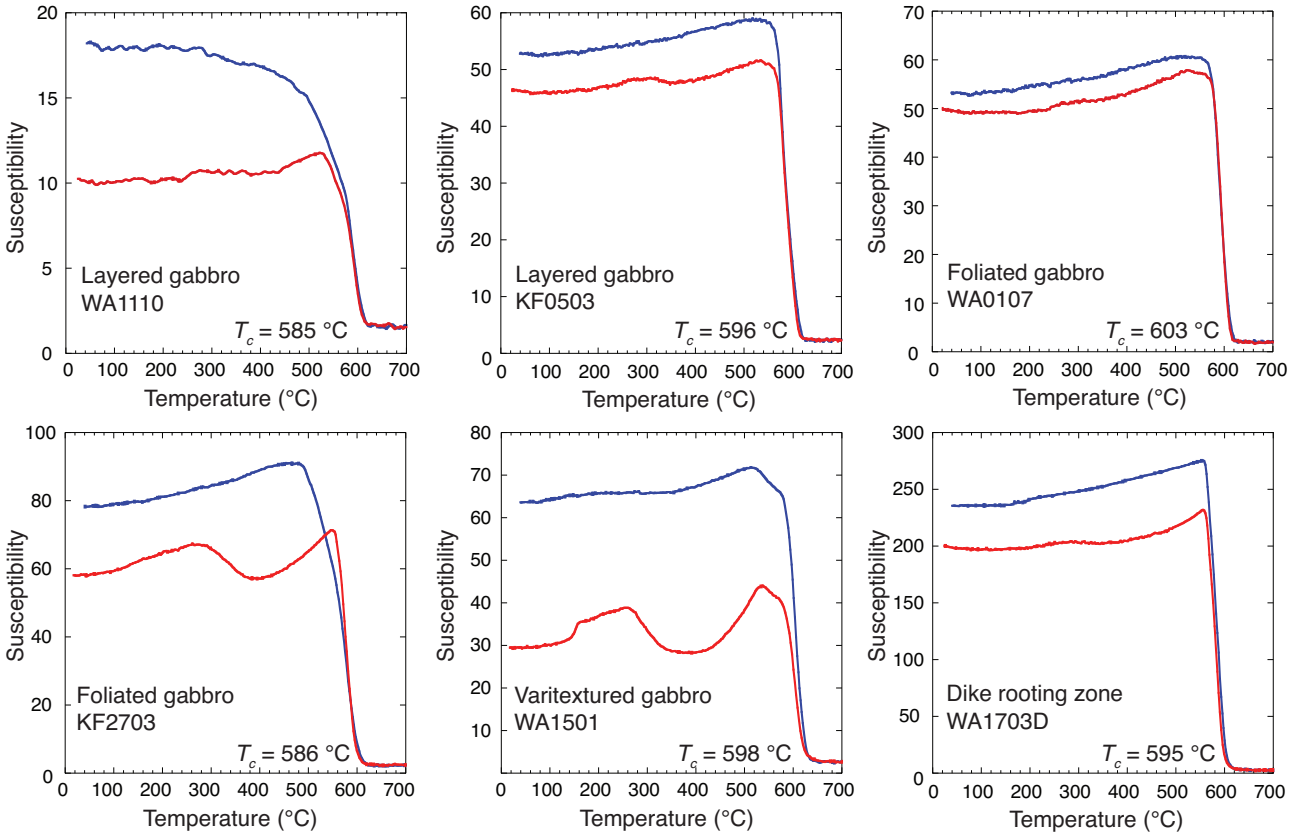

Figure DR9. Respresentative examples of the variation of low field magnetic susceptibility with temperature for lower crustal rocks from Wadi Abyad (WA) and Wadi Khafifah (KF) in the Oman ophiolite. Red = heating curves, blue = cooling curves. Tc = Curie temperature, calculated using the inverse susceptibility method of Petrovsky & Kapička (2006). Curie temperatures of 585-600°C indicate that magnetite is the dominant magnetic carrier in these rocks, but bumps in heating curves at lower temperatures in some samples may indicate alteration of titanomagnetite to titanomaghemite as a result of low-temperature oxidation and/or changes in susceptibility resulting from thermal annealing of stresses in magnetite. Increased susceptibility upon cooling indicates production of magnetite during heating.

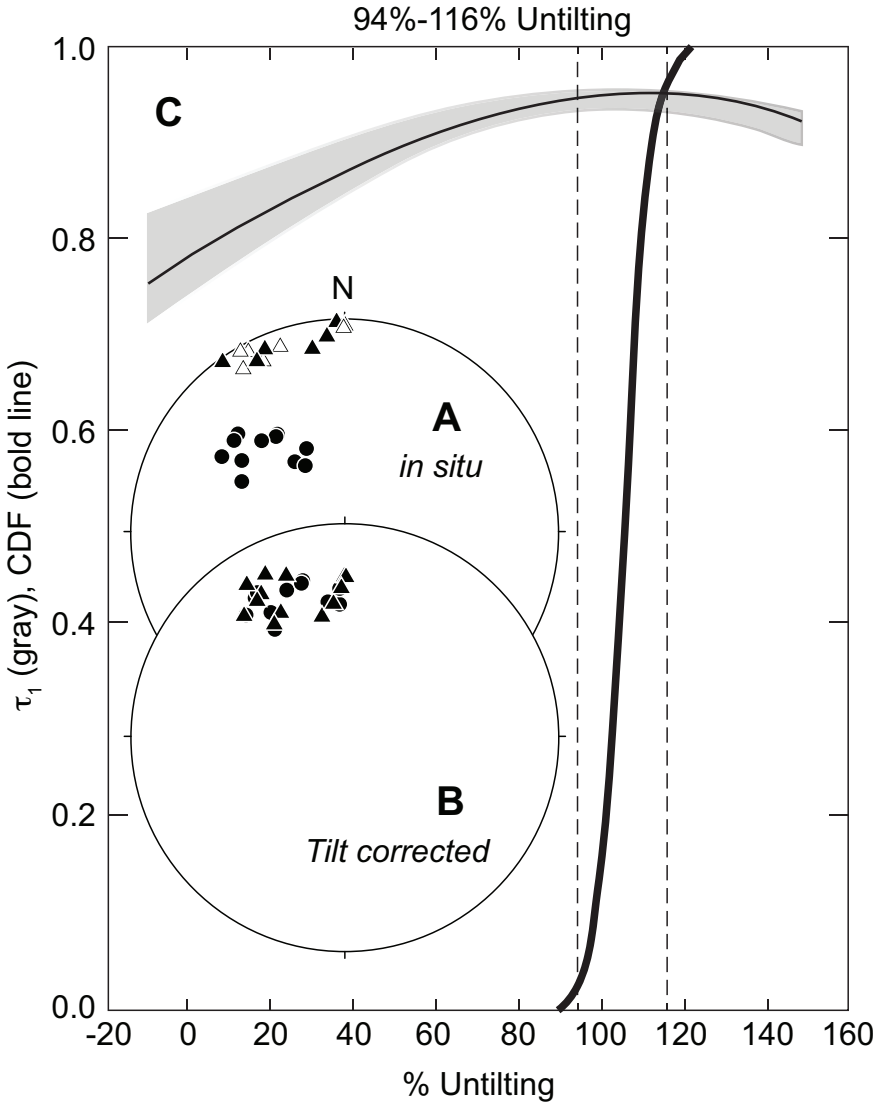

Figure DR10. A: Equal area projection of *in situ* site mean directions of magnetization from layered and foliated gabbros from Wadi Abyad (circles; excluding sites WA09-11) and Wadi Khafifah (triangles). B: Data from A after restoring the Moho to horizontal at each locality. C. Positive bootstrap fold test (Tauxe and Watson, 1994) demonstrating remanence acquisition prior to tilting in these sections. Gray region contains the trends of the largest eigenvalues (τ_1s) of orientation matrices from representative pseudo-samples drawn from A during progressive untilting. Bold line is the cumulative distribution of 1000 maxima of τ_1 and dashed lines are the bounds that enclose 95% of them.